Indian journal of
Engineering

Numerical and Experimental Study of UHPC Beams with Square and Rectangular Openings Reinforced with Steel Plates

Hayder SH Hudaib[1]*, Hayder MJ Al-Khafaji[2]

To Cite:
Hudaib HSH, Al-Khafaji HMJ. Numerical and Experimental Study of UHPC Beams with Square and Rectangular Openings Reinforced with Steel Plates. *Indian Journal of Engineering*, 2026, 23, e9ije1721
doi:

Author Affiliation:
[1]Civil Engineering Department, College of Engineering, University of Babylon, Babylon, 51001, Iraq.
[2]Civil Engineering Department, College of Engineering, University of Babylon, Babylon, 51001, Iraq.

Corresponding author:
Hayder SH Hudaib,
Engineering Department, College of Engineering, University of Babylon, Babylon, 51001, Iraq. E-mail: haider.saad2016@gmail.com

Peer-Review History
Received: 21 November 2025
Reviewed & Revised: 27/December/2025 to 30/July/2026
Accepted: 09 August 2026
Published: 21 August 2026

Peer-Review Model
External peer-review was done through double-blind method.

Indian Journal of Engineering
pISSN 2319–7757; eISSN 2319–7765

DISCOVERY SCIENTIFIC SOCIETY

ABSTRACT

In the present work an integrated experimental and computational method is used to explore the structural performance of ultra-high-performance concrete (UHPC) beams with square and rectangular transverse web apertures reinforced with externally bonded steel plates. Five UHPC beam specimens were examined under four-point bending, consisting of a control beam, beam with a square opening, a beam with a rectangle opening, and their corresponding reinforced specimens. A three-dimensional nonlinear finite element model was created in Abaqus to mimic the nonlinear behavior, crack growth and interaction between the UHPC and the external strengthening system. The experimental results showed that the internal force transfer mechanism was severely disturbed by the openings, and the stress concentration around the opening boundaries was localized, which caused the ultimate load capacities of the beams with square and rectangular openings to decrease by approximately 11.0% and 11.7%, respectively, compared with those of the control beam. The rectangular hole with elongated shape and larger interruption of the stress flow led to more severe stiffness degradation and fracture localization. The externally bonded steel plates increased the load-carrying capacity, slowed the fracture propagation, and improved the stress redistribution, significantly enhancing the structural response. The reinforced square-opening beam had a little higher capacity than the control specimen, while the strengthened rectangular-opening beam showed partial structural recovery. The computational predictions were in excellent accord with the experimental data in terms of load-deflection response, fracture patterns and ultimate load capacity. The results confirmed that the steel plate strengthening is an efficient rehabilitation approach for UHPC beams with web apertures nevertheless the strengthening efficiency largely depends on the opening shape.

Keywords: ultra-high-performance concrete (UHPC), Square and Rectangular Openings, Steel Plates Reinforcement.

1. INTRODUCTION

Ultra-high-performance concrete (UHPC) has become a very promising cementitious composite in modern infrastructure over the last several decades.

UHPC has a dense microstructure and contains dispersed steel fibers that provide outstanding mechanical and durability characteristics (Huang and Yao 2024; Richard and Cheyrezy 1995; Yang et al., 2022). UHPC may be formulated to achieve very high compressive strengths, although practical structural applications of UHPC will often employ intermediate strength levels depending on design requirements. The integrated steel fibres are particularly crucial to its performance, as they actively seal micro-cracks and provide long-term post-cracking tensile strength, considerably enhancing the ductility, toughness and total load-bearing capacity of flexural parts. Therefore, UHPC is becoming an increasingly promising alternative for making durable and optimized beams with superior crack control (Zhu et al., 2023; 2024).

The combination of the utility systems needed (HVAC) ducts, water pipes, and electrical conduits) and the structural components has become a standard in current building construction. This is usually achieved by opening up transversely in beams to maximize the use of space and to meet architectural requirements (Kartal and Kısıklı 2024; Özkılıç et al., 2023). The presence of such openings, however, leads to geometric discontinuities which bring about a significant transformation in the flow of internal forces in the beam. These discontinuities lead to the loss of stiffness, flexural capacity, and structural efficiency in general, although the discontinuities are not in the critical shear areas (Al-Enezi et al., 2023; Taher, 2024). The existence of openings has been reported to change the distribution of stress and cause local tensile damage at their boundaries, thus increasing the rate of crack initiation and propagation (Al-Sheikh, 2014; Sathiyapriya et al., 2021). In addition, the opening geometry significantly influences the structural behavior in general. Circular openings are more likely to redistribute stress than square and rectangular openings that add sharp edges that cause extreme stress concentration, leading to local cracking and increased losses in load-carrying capacity. Of these, rectangular openings are said to have a worse impact on strength than square ones because of their long shape and greater perturbation of internal force paths (Al-Sheikh, 2014). Moreover, large openings can lead to Vierendeel-like mechanisms, which can be highly effective in influencing the crack patterns and redistribution of stress in the beam (Aykac et al., 2013).

To mitigate the adverse structural effect of web openings many approaches of strengthening have been developed and they are extensively utilized in particular in classic reinforced concrete buildings. One such option is strengthening by externally bonded steel plate which has been shown as a practical and efficient means of restoring the structural capacity. Bonded steel plates are used to increase the stiffness, redistribute the stress and reduce stress concentration around the opening and reduce crack propagation rate and increase the ultimate load carrying capacity of beams (Adhikary and Mutsuyoshi, 2002; Hamoda et al., 2024; Kholil and Ahmed, 2026). These strengthening systems can be beneficial in reducing the localization of stress around openings and localized damage, resulting in better structural behavior and more controlled crack propagation, as observed in the stress concentration and cracking behavior in beams with openings (Andoh et al., 2025; Branesh Robert et al., 2021), which has been shown experimentally and numerically. Furthermore, externally bonded strengthening is used to increase the stiffness and load-bearing capacity in the event of adequate bond interaction between the steel plate and the concrete surface (Kholil and Ahmed, 2026). In spite of these developments, the majority of the available studies have been done on conventional concrete, yet the performance of UHPC beams with openings, especially sharp-cornered geometries, is not well comprehended. Moreover, the interplay between external strengthening of steel plates and the internal fiber-bridging mechanism of UHPC is not completely comprehended.

This paper presents a detailed experimental and computational examination on the flexural behaviour of ultra-high-performance concrete (UHPC) beams with sharp-cornered square and rectangular web apertures strengthening with externally bonded steel plates. This study carefully investigates the effect of opening geometry on structural performance, fracture formation and stress redistribution, unlike earlier studies which mainly focused on conventional reinforced concrete or circular openings. A three-dimensional nonlinear finite element model with the formulation of Concrete Damage Plasticity (CDP) and the cohesive interface modeling is created and verified with the experimental findings, which can predict the load-deflection behavior and damage propagation accurately. Moreover, the study clarifies the interaction between the inherent fiber-bridging ability of UHPC and the external reinforcement by the steel plate, showing the geometry-dependent performance of the strengthening technique, and offering useful information for the design and rehabilitation of UHPC structural members with transverse web openings.

In order to address this literature gap, the present study investigates the structural performance of ultra-high-performance concrete (UHPC) beams with transverse square and rectangular web openings strengthened with externally bonded steel plates. In contrast to circular openings, sharp-cornered openings can create large stress concentrations that affect the mechanisms of crack initiation and propagation. To determine the effect of opening geometry on the load-deflection response, crack patterns, and failure modes of the beams, an experimental program was carried out with nonlinear finite element modeling. The main aim of the research is to investigate the efficacy of steel plate strengthening in recovering the structural performance of UHPC beams that have been weakened by such discontinuities. The results of this research are likely to be of practical use in designing and strengthening UHPC structural members with transverse openings.

2. MATERIALS AND METHODS

Materials and UHPC Mix Design

The ultra-high-performance concrete (UHPC) used in this study was made by mixing fine materials only to obtain a dense and homogeneous matrix. The mixture did not contain coarse aggregates as in conventional concrete to enhance the packing of the particles and the mechanical performance. The binder system was mainly composed of sulfate-resistant Portland cement mixed with silica fume (MS 610), which was added to enhance the microstructure and to enhance the compressive strength of the concrete. The main aggregate phase was fine sand that had passed through the 0.6 mm sieve and quartz sand that had a size between 0.3 and 0.7 mm. Since UHPC mixtures usually demand a very low water-to-binder ratio, a high-range polycarboxylate-based superplasticizer was incorporated to provide sufficient workability during mixing and casting. The ratio of water to binder used in this experiment was about 0.16. The tensile resistance was enhanced by adding a volume fraction of 2% steel fibers to enhance the post-cracking behavior of the concrete. The length of the fibers was 13 mm and the diameter was 0.2 mm, which gave an aspect ratio of about 65. These fibers play a major role in crack bridging and enhance the ductility of the UHPC matrix. Table 1 summarizes the proportions of the UHPC mixture used in the experimental program.

Table 1. UHPC Mix Proportions

Material	**Quantity (kg/m³)**
Cement	950
Quartz Sand	840
Quartz Powder	210
Silica Fume	190
Water	188.67
Superplasticizer	44.07
Steel Fibers	157

The dry constituents were mixed first to allow a uniform distribution. Water and superplasticizer were then added slowly as the mixing process proceeded. Lastly, the mixture was gradually mixed with steel fibers to prevent the clustering of fibers and to maintain even distribution of the fibers in the concrete. The specimens were covered after casting to avoid loss of moisture. The molds were removed after about 24 hours, and the specimens were then kept in laboratory conditions until the age of testing. Standard laboratory tests were used to determine the mechanical properties of the UHPC. The mean compressive strength of 70 mm cube specimens was about 122 MPa, and the mean splitting tensile strength was 14.67 MPa.

Beam Specimens and Reinforcement Arrangement

Five UHPC beams were made and tested to examine the effect of transverse openings on structural performance. The overall dimensions of all specimens were the same, the beam length was 1600 mm, and the cross-section was rectangular, 150 mm wide and 250 mm deep as shown in Figure 1. The same dimensions were utilized to allow a direct comparison of the different beam designs. All beams were designed with the same longitudinal reinforcement to provide the same flexural capacity. Two 12mm diameter reinforcing bars were employed for the tension zone and two 8mm diameter bars (mostly used for stabilization of the reinforcement cage during casting) for the compression zone. Shear reinforcement was provided with closed stirrups of 8 mm diameter with a spacing of 100 mm along the beam length. This reinforcement arrangement was chosen to avoid premature shear failure and to make sure that the predominant failure mode would be flexural. Mechanical properties of reinforcing steel were taken based on standard tensile tests that were reported on bars manufactured by the same manufacturer and grade (Kazem and Al-Zahra, 2025). The average yield strength of the bars of 8 mm was about 486 MPa whereas the bars of 12 mm had an average yield strength of around 500 MPa. For a fair comparison, the square opening (90 × 90 mm) and the rectangle opening (65 × 130 mm) were chosen to have about identical opening areas (difference < 5%), such that the effect of the opening size was minimized and the structural reaction seen was mostly due to the opening geometry.

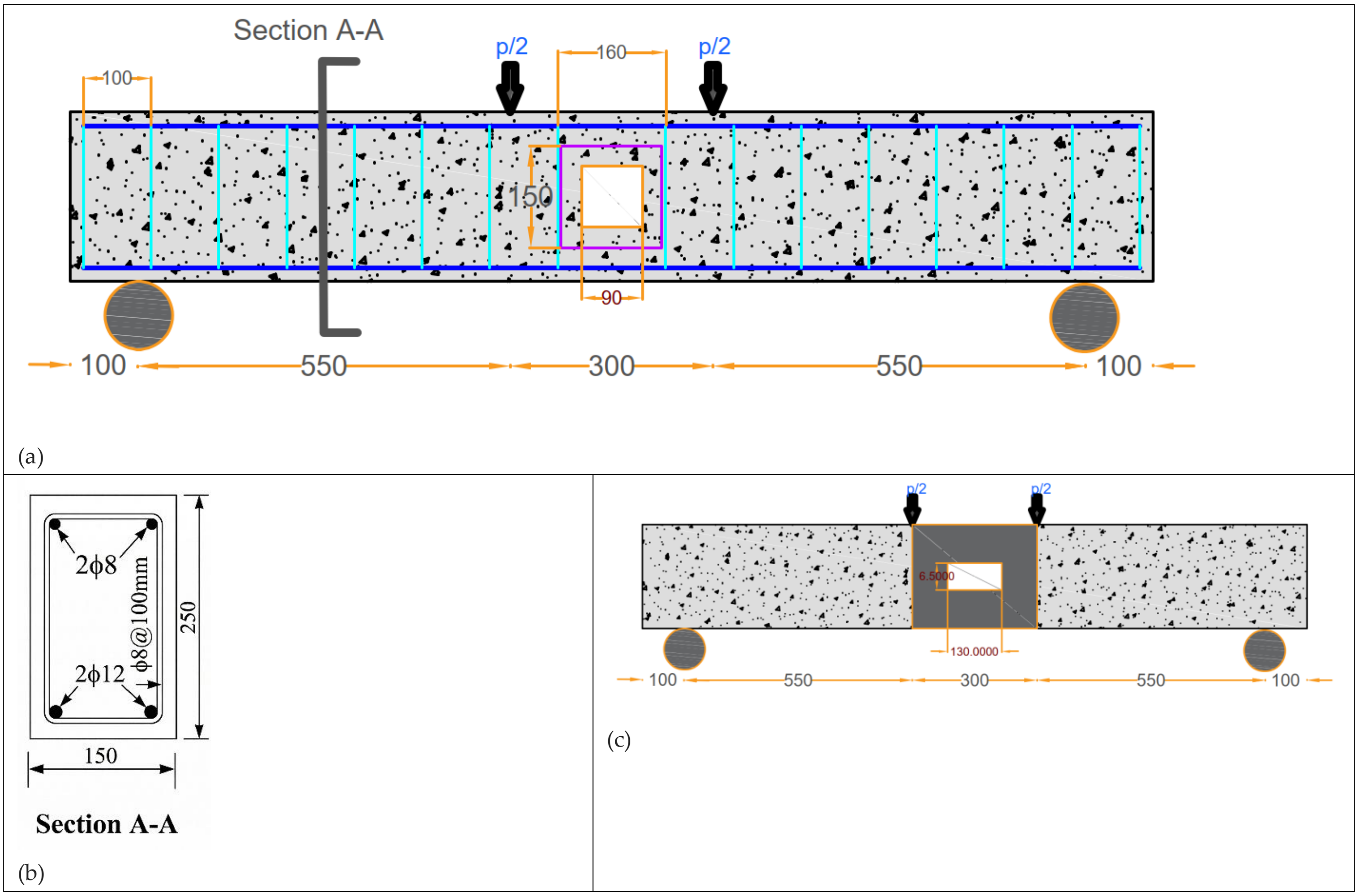

Figure 1. (a) strengthening configuration for the square opening specimen (SOS), (b) reinforcement details at Section A–A, and (c) strengthening configuration for the rectangular opening specimen (ROS).

The present investigation considered three beam configurations:

Control Beam (CB)

The initial specimen was cast without any opening and was used as the control beam. The specimen was used to test the structural behavior of UHPC beams in four-point bending as the baseline.

Beams with Opening

To examine the effect of the geometry of openings on the structural behavior, four beam specimens were made with transverse openings at the midspan in the constant moment region. Additional closed stirrups were used to provide local confinement reinforcement around the openings to control crack development and improve the local structural response.

Square opening (SO)

The square opening specimen (SO) was provided with an opening size of 90 mm × 90 mm with additional closed stirrups of 150 mm × 150 mm provided around the opening area.

Rectangular opening (RO)

The rectangular opening specimen (RO) had an opening of 65 mm × 130 mm. The confinement reinforcement surrounding the opening was made of closed stirrups that were 150 mm × 160 mm. The openings were correctly cast, and there was no horizontal movement, which guaranteed the similarity between the experimental setup and the numerical model.

Strengthened Beams with square and rectangular Openings (SOS & ROS)

In addition to the unstrengthened specimens, two reinforced beams were also fabricated to test the efficiency of externally bonded steel plates to restore the structural performance of UHPC beams with sharp-cornered web holes. Commercially available mild steel plates (300 mm × 250 mm × 1 mm) were symmetrically bonded to both sides of the beam on the opening area using a two-component structural epoxy adhesive, Sikadur®-31 CF Slow. The specified plate dimensions were enough to completely cover the aperture and the surrounding stress concentration zone, and so provided enough anchoring length for efficient redistribution of stress and minimized the possibility of premature debonding of the plate (Table 2). The concrete surfaces were cleaned and roughened prior to bonding to increase the mechanical interlock and to improve the performance of the glue. The epoxy glue was placed in a thin, continuous and evenly dispersed coating. The steel plates were then physically clamped until full curing. Although the thickness of the adhesive layer was not empirically determined but every possible effort was taken to ensure a consistent bond line during specimen preparation. The steel grade and yield strength were not experimentally evaluated as commercially available mild steel plates were used for practical laboratory application and they are considered a limitation of the current research. The strengthening configuration chosen was drawn from successful experimental applications published in the literature and validated by preliminary laboratory experiments. The optimization of the plate dimensions by analytical design processes was out of the scope of the present work.

Table 2. Mechanical Properties of Sikadur®-31 CF Slow Adhesive

Property	Value
Product	Sikadur®-31 CF Slow
Adhesive type	Two-component structural epoxy adhesive
Density	1.93 kg/L
Compressive strength (7 days)	52–54 MPa
Tensile strength	≈13 MPa
Flexural tensile strength	≈27 MPa
Tensile modulus of elasticity	≈3000 MPa
Compressive modulus of elasticity	≈2600 MPa
Tensile adhesion to concrete	>4 MPa (100% concrete failure)
Tensile adhesion to steel	≈15 MPa
Mixing ratio	2:1 (Part A : Part B by weight)

Experimental Test Setup

The beam specimens were all tested under four-point bending conditions with a hydraulic loading frame. The supports were simply supported with a clear span of 1400 mm between them. Symmetrical loading of the beam was applied using steel loading plates on the top surface. The distance between the two load points was 300 mm, which formed a constant bending moment area at midspan where the openings were. The load points were placed 550 mm away from the closest support. The load was progressively applied under load-controlled conditions until failure took place. The midspan deflection was also measured during testing with a Linear Variable Differential Transformer (LVDT) at the beam center. The test also monitored crack initiation and propagation visually during the test to determine the dominant failure mode and the effect of the openings on the structural response.

3. RESULTS & DISCUSSIONS

Numerical Modeling

The behavior of the tested UHPC beams was simulated by developing a three-dimensional nonlinear finite element model with Abaqus/Standard. The modeling method was taken from a proven numerical study (Kadhim et al., 2021), but with certain changes to the material properties and conditions of the current study. The numerical model was built to reproduce the shape, reinforcement configuration and loading conditions used in the experimental program. The model was first evaluated on the control beam, then used for further research. The numerical study was performed in an effort to get more information on the distribution of stresses, development of damage and propagation of cracks in beams with transverse holes. The numerical model was validated against the experimental results of the control beam for the load-deflection response and the ultimate load capacity and was then expanded to study the beams with openings and strengthening configurations. This test proved the ability of the model to properly represent the nonlinear behavior of UHPC beams.

Geometry and Finite Elements

The numerical model geometry was the same as the experimental beams and had a cross-section of 150 mm × 250 mm and a total length of 1600 mm as shown in Figure 2. The UHPC body was modeled using eight-node linear brick elements with reduced integration (C3D8R). The selection of this element type was motivated by its good trade-off between numerical accuracy and computing economy for nonlinear analysis of concrete. Reduced-integration solid elements have been widely tested in finite element simulations of reinforced concrete and UHPC. They are capable of capturing cracking, deterioration of the stiffness and development of damage with a reduced computing cost and without severe numerical locking.

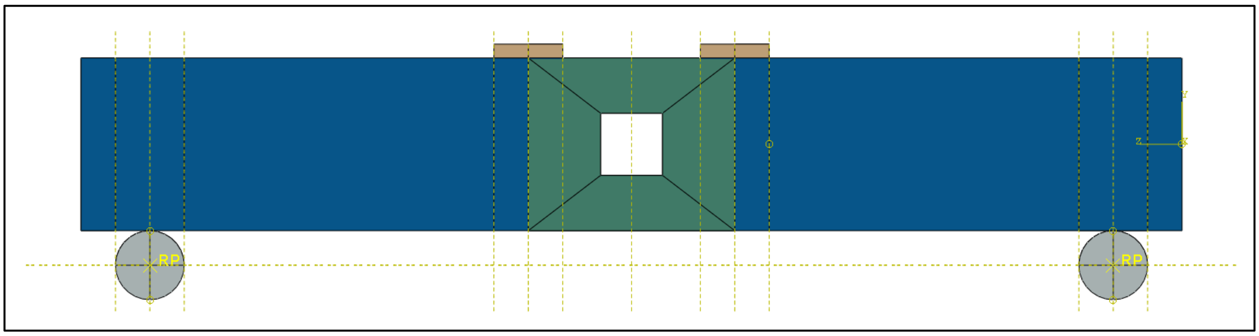

Figure 2. Finite Element Model

Most parts of the beam were modeled with a mesh size of 25 mm. Mesh refinement was, however, done in areas where high stress concentration was likely to occur, especially at the loading points and around the openings as shown in Figure 3. The mesh size in these regions decreased to about 15 mm, and an even finer mesh of about 5 mm was employed around the boundaries of the openings to better resolve localized damage. A mesh sensitivity analysis was done to make sure that the numerical results were not highly dependent on the mesh size. The mesh size surrounding the opening was also decreased to 3 mm instead of 5 mm, and the resulting difference in the final load was observed to be less than 2%, which means that the mesh density applied is correct and at the same time the efficiency of the computation is not very high.

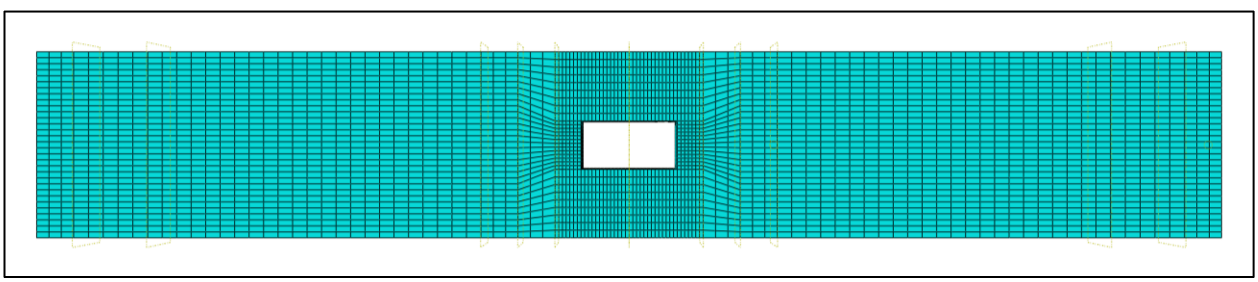

Figure 3. Mesh Distribution

Material Modeling

In this work, the UHPC was experimentally characterized by compressive strength, splitting tensile strength and flexural tensile strength tests. The average compressive strength of the UHPC was 122 MPa, while the average splitting tensile strength was 14.67 MPa. The characteristics obtained experimentally served as the main material parameters for the assessment of the structural response of tested beams (Fakeh et al., 2025; Kadhim et al., 2021). The direct tensile strength, elastic modulus, fracture energy and fiber orientation were not measured experimentally, since they were outside the scope of the current experimental program. For the numerical simulations, the elastic modulus and tensile strength were estimated using known empirical relationships based on the experimentally measured compressive strength and the compressive and tensile stress–strain relationships including the post-peak softening response were taken from validated constitutive models reported in the literature and subsequently calibrated to match the measured compressive strength. Moreover, the Concrete Damage Plasticity (CDP) parameters were used from previously confirmed UHPC numerical studies. Since all specimens were created using the same ingredients, mixing techniques, casting methods and curing conditions, the distribution of fibers was considered to be uniform with random orientations throughout the whole numerical analysis (Table 3). This assumption is typically used in finite element simulations of UHPC when direct measurements of fiber orientation are lacking. The modulus of elasticity was determined based on the empirical relationship that was assumed in the reference model:

$$E = 3840\sqrt{f_c'} \quad (1)$$

Elastic modulus was considered to be 42.4 GPa and the Poisson's ratio was considered to be 0.18.

A bilinear stress-strain relationship was used to characterize the tensile behavior of UHPC to model crack initiation and post-cracking softening. The tensile strength was determined based on the empirical relationship borrowed in the reference study:

$$f_t = 0.55\sqrt{f_c'} \quad (2)$$

The model consists of an initial elastic behavior and a second tensile softening due to cracking and fiber-bridging effects (Kadhim et al., 2021).

Table 3. Mechanical properties used in the numerical model

Property	UHPC	Steel reinforcement	Steel plate
fc'	122 MPa	—	—
Ft	6–7 MPa	—	—
E	42.4 GPa	200 GPa	200 GPa
N	0.18	0.3	0.3
Fy	—	486–500 MPa	—

Figure 4 indicates compressive and tensile stress-strain relationships which are utilized in the numerical model. The compressive behavior is nonlinear and has a downward branch to explain post-peak softening, and the tensile behavior is bilinear to explain crack initiation and progressive softening by fiber bridging.

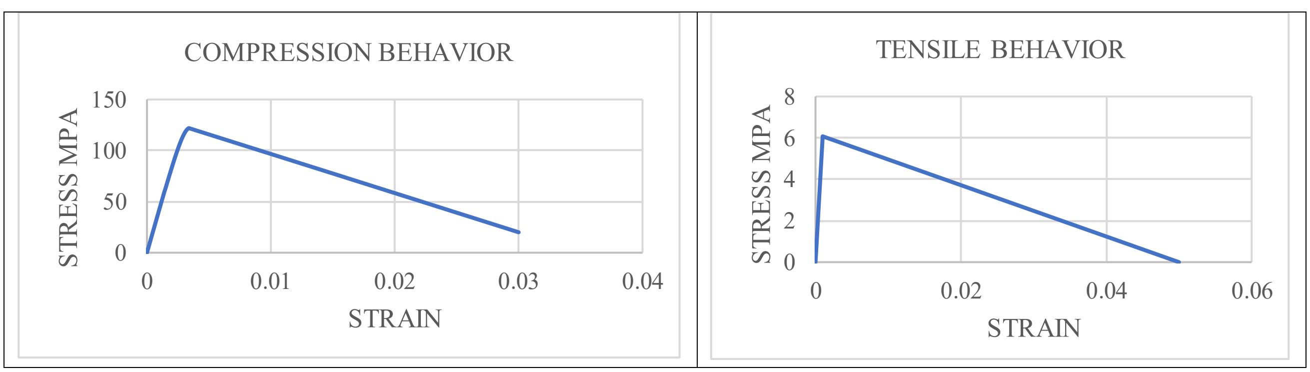

Figure 4. Stress–strain models for UHPC

The tensile softening branch that had intermediate points was introduced to provide numerical stability and reduce abrupt changes in stiffness. The CDP model parameters (dilation angle, eccentricity, viscosity parameter, and strength ratios) were selected based on the previous numerical studies of UHPC and the recent calibration recommendations that are found in the literature (Fakeh et al., 2025; Kadhim et al., 2021). The selected parameters will be used to appropriately model the damage development, steady convergence, and realistic nonlinear response to loading.

The CDP parameters used in this research were chosen from previously verified numerical studies on UHPC and calibrated with the tested control beam. Initially, ranges of parameters provided in the literature were taken into account, and then many trial analyses were undertaken to get the closest agreement between the numerical and experimental load–deflection responses (Table 4). The best agreement between experimental and numerical results was achieved for a dilation angle of 36° among the studied parameter combinations, although greater values of dilation angle are often reported in earlier research. Therefore, the calibrated parameter set (ψ = 36°, eccentricity = 0.1, fb0/fc0 = 1.16, K = 0.667 and viscosity = 0.0008) was used for all beam models without any further change, so as to maintain consistency throughout the whole numerical study.

Table 4. CDP parameters

Parameter	Value
Dilation angle	36
Eccentricity	0.1
fb0/fc0	1.16
K	0.667
Viscosity	0.0008

The reinforcement bars were modeled as embedded elements with an elastic-perfectly plastic constitutive model as shown in Figure 5. Elasticity of steel was considered as 200 GPa and Poisson's ratio was considered as 0.3 which are the normal values in reinforced concrete model (Kadhim et al., 2021).

Figure 5. Details of Steel Reinforcement.

Boundary Conditions and Loading

In order to replicate the experimental setup, the beams were simulated as simply supported members. All the degrees of freedom of translation were restrained at the first support (U1 = U2 = U3 = 0), and the second support was free to move longitudinally to prevent artificial axial restraint (U2 = 0). The model had steel loading plates at the load application points to make the load more realistic. The loading force was exerted by a vertical displacement that was applied at the loading points. Displacement control was used to apply the loading, and the maximum displacement imposed at the loading points was 50 mm vertically. To compare the numerical response with the experimental results, the numerical response was assessed until the displacement at which each specimen failed in the experiment. It was analyzed using a Static General analysis step that was automatically incremented. The initial increment was set to 0.01 and a minimum increment of 1×10^{-6} and a maximum increment of 0.1 to guarantee the stability of convergence in the nonlinear analysis. The nonlinear geometry effects (NLGEOM = ON) were considered.

Modeling of Transverse Openings and Strengthening

This study carries out finite element numerical simulations of ultra-high-performance concrete (UHPC) beams. In an effort to properly account for stress redistribution and damage development due to the presence of transverse openings, two kinds of opening configurations are explicitly included in the geometric model: a square opening of 90mm×90mm and a rectangle opening of 65mm×130mm. The opening borders are improved mesh discretized to increase the accuracy of stress prediction and crack localization in the crucial zone surrounding the openings where stress concentration and nonlinear damage are prone to occur. This research also specifically simulates the mechanism of externally bonded steel plate reinforcement. The bonding activity of Sikadur®-31 CF is simulated via a surface-based cohesive interaction. Slow epoxy glue at steel plate and concrete interface; this is modeled using the mature technique in current literature (Kholil and Ahmed, 2026).

The reinforcement plate uses the four-node reduced integration shell element (S4R), and the bond interface is assigned an equivalent thickness of 2mm consistent with actual engineering practice, to evaluate the performance improvement and stress transfer effect of the reinforcement system. The bond interaction was governed using a traction–separation constitutive relationship, where the normal and shear stiffness parameters were defined according to the elastic properties of the epoxy adhesive using $K_{nn} = E/t$and $K_{ss} = G/t$to ensure realistic load transfer across the interface (Kholil and Ahmed, 2026). The damage initiation in the adhesive layer was modeled by a nominal stress criterion, and the progressive degradation of the interface was described by an energy-based damage evolution approach, with calibrated fracture energies of 0.2 N/mm and 0.3 N/mm in normal and shear modes, respectively. In addition, a tiny viscosity parameter was incorporated to enhance numerical stability and convergence throughout the nonlinear softening process. The finite element model was verified against the experimentally tested control beam and then extended to the beams with web apertures and strengthening techniques. The same constitutive models, CDP parameters, interaction characteristics and meshing approach were used for all the remaining specimens with no change after successful validation. The verification approach includes a direct comparison between computational and experimental load–deflection curves, ultimate load capacities, failure mechanisms and fracture patterns. The good agreement between numerical predictions and actual observations demonstrates that the selected modeling technique can reliably reflect the nonlinear structural behavior of UHPC beams with transverse openings and externally bonded steel plate reinforcement.

Load–Deflection Response

The experimental load-deflection curves of the five beams tested, i.e., the control beam (CB), the beam with a square opening (SO), the strengthened square-opening beam (SOS), the beam with a rectangular opening (RO), and the strengthened rectangular-opening beam (ROS), are shown in Figure 6. Overall, the initial almost linear behavior of all specimens was followed by a nonlinear phase, which was related to crack formation and loss of stiffness, and then a post-peak decreasing branch, which is typical of flexural behavior of reinforced concrete beams as described in earlier literature (Al-Enezi et al., 2023; Kartal and Kısıklı, 2024). Transverse openings resulted in a decrease in stiffness and load-carrying capacity, and externally bonded steel plates helped to enhance the structural behavior, the effectiveness of which depended on the shape of the opening. The control beam (CB) showed the best reference behavior of the unstrengthened specimens with an ultimate load of 186.5 kN. The curve exhibited a steady increasing branch and then a slow post-peak softening response, which is in line with the ductile flexural behavior that is typically linked with UHPC beams that have steel fibers. The ultimate load of specimen SO was decreased to 166.05 kN by the introduction of a square opening, which is a decrease of about 11.0% compared to the control beam.

Besides the strength decrease, the SO beam exhibited a smaller stiffness at the post-cracking stage and a more significant degradation in the post-peak stage. This action can be explained by the fact that the internal force path was interrupted and stress concentration was formed at the corners of the square opening. The same was the case with the beam with the rectangular opening (RO), which attained aی ultimate load of 164.7 kN, a decrease of approximately 11.7% of the control beam. The rectangular opening had the lowest load capacity of the unstrengthened beams with openings. This reaction suggests that the rectangular opening resulted in a more unfavorable disturbance in the stress transfer and facilitated earlier degradation of stiffness, probably due to the joint impact of sharp corners and the greater dimension of the opening in a single direction. The externally bonded steel plates used to strengthen the square-opening beam greatly enhanced the structural response. The ultimate load of the strengthened specimen (SOS) was almost 1.4% greater than that of the control beam and almost 14.0% greater than that of the similar unstrengthened specimen SO. SOS also showed improved stiffness and a more stable after-peak response in the load-deflection curve, indicating that the steel plates were effective in redistributing the stresses around the opening and mitigating the adverse impact of stress concentration at corners.

The strengthened rectangular-opening beam (ROS) was also better than the unstrengthened one. It had an ultimate load of 172.1 kN, approximately 4.5% higher than that of specimen RO. However, the strengthened beam with the rectangular opening was still about 7.7% less than the control beam. These findings indicate that the steel plate strengthening improved the performance of the beam, but the rectangular opening still had a drawback compared to the square one, and the improvement was not as significant as that of specimen SOS. In general, the experimental curves indicate that the shape of the opening had a definite impact on the flexural response of UHPC beams. The square and rectangular openings decreased the load-carrying capacity relative to the control beam, and the decrease was partially or completely offset by strengthening with steel plates. The best performance of the opened beams was recorded in the strengthened square-opening specimen, with the unstrengthened rectangular-opening beam recording the least response.

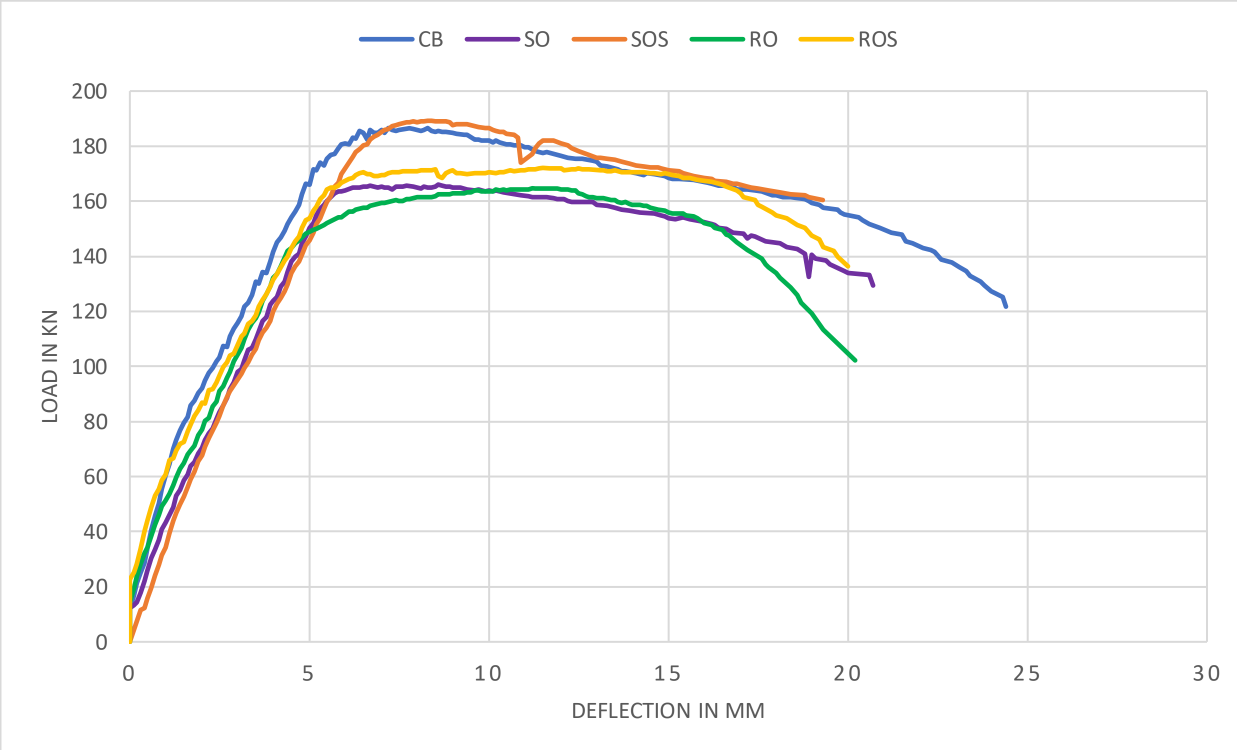

Figure 6. Load–Deflection Curves

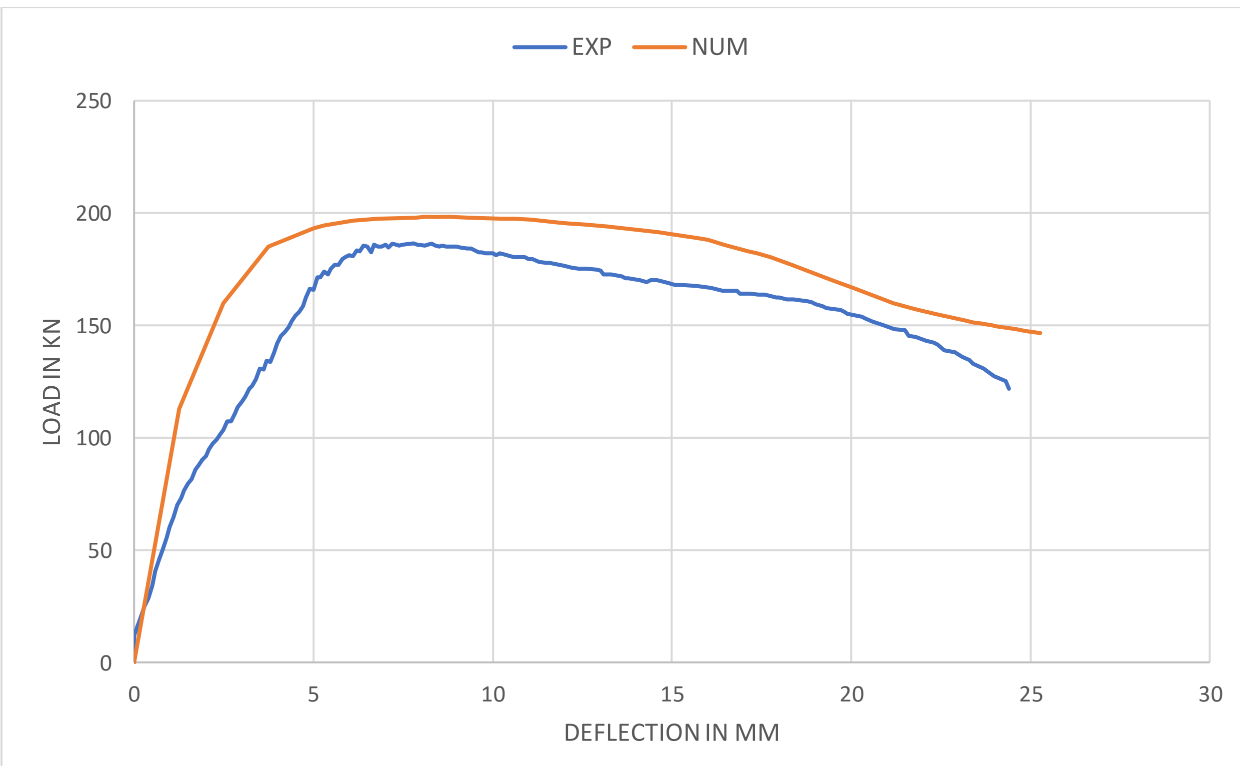

Figure 7. Load–Deflection Curve for CB sample

Control Beam (CB)

The ultimate load of the control beam was 186.5 kN and the finite element model gave a slightly higher value of 198.233 kN, and the difference between them was around 6.3% as shown in Figure 7. This is a rather small difference and demonstrates a good agreement between the experimental and numerical data. The final deflection at failure that was experimentally recorded was about 24.4 mm. The initial observable cracking load on the control beam was 40 kN. To compare, the cracking loads of the other specimens were 30 kN in the square opening beam, 20 kN in the rectangular opening beam, 60 kN in the strengthened square specimen, and 40 kN in the strengthened rectangular specimen. It is worth noting that, in the strengthened specimens, the cracks in the areas covered by the steel plates could not be visually observed during testing. Thus, the measured cracking loads are the first visible cracks that are seen outside the strengthened areas. This is due to the redistribution of stress and local stiffening effects that the strengthening system offers, delaying crack initiation and altering the crack propagation paths as observed in earlier works on strengthened beams with openings (Almusallam et al., 2018; Morsya and Barima, 2019). The load-deflection response was nearly linear at the beginning of cracking. Once cracked, there was a progressive decrease in stiffness as a result of crack development and propagation. In addition to the peak load, the beam exhibited a ductile flexural response and then a steady descending branch, which means that the failure mode was dominated by flexure. The crack pattern observed was typical flexural behavior. The cracks started in the bottom tension zone at midspan and extended upwards to the compression area. The cracks became very wide as the load increased until the beam attained its final load.

Beam with Square opening (SO)

The ultimate load of specimen SO was reduced to 166.05 kN with the addition of the square opening, which is a decrease of about 11.0% of the experimental ultimate load of the control beam as shown in Figure 8. The ultimate load was predicted to be 186.197 kN by the finite element model, which is about 12.1% different from the experimental value. The load-deflection behavior of specimen SO exhibited a lower initial stiffness compared to the control beam with a higher localized deformation in the area of the opening. This tendency can be explained by the fact that the natural load path is disrupted by the square opening and stress concentration is formed at its sharp edges, as it was reported in the previous studies (Almusallam et al., 2018; Hussein et al., 2020; Morsya and Barima, 2019). Cracking started in the bottom tension zone and moved upwards with the increase in load. It was found that the presence of the opening affected the crack path although flexure remained the predominant structural response. The prevailing crack was more likely to lean towards the opening rather than spread vertically. The inclined crack pattern is attributed to the change in the stress distribution around the opening and the change in the internal force paths as a result of the geometric discontinuity of the square opening. This has been observed in beams with openings, where diagonal cracks are often formed at the corners (Hussein et al., 2020; Morsya and Barima, 2019). The ultimate deflection at failure was approximately 20.7 mm, which is less than that of the control beam. Moreover, the post-peak branch had a steeper downward slope, which showed a decrease in ductility and faster crack propagation in the weakened area surrounding the opening as a result of stress concentration effects (Almusallam et al., 2018; Hussein et al., 2020).

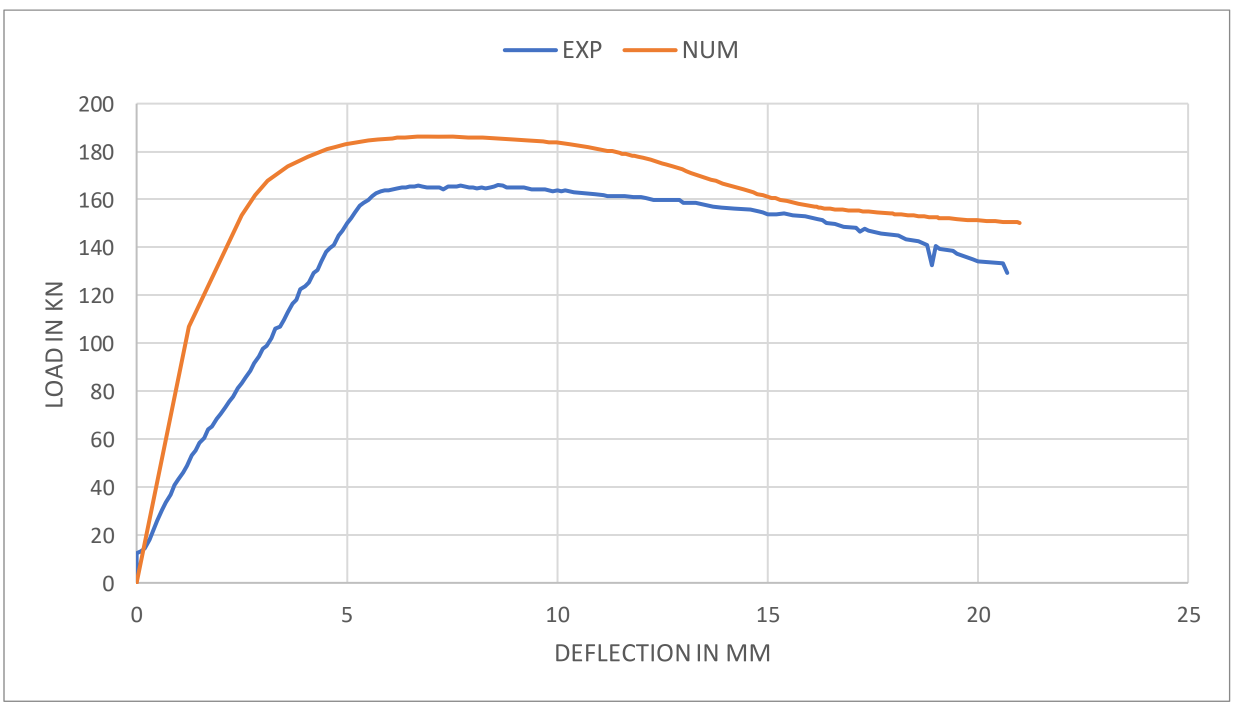

Figure 8. Load–Deflection Curve for SO sample

Beam with Square opening Strengthened using Steel Plate (SOS)

Figure 9 shows that external steel plates strengthened the square hole of specimen SOS, improving its structural response. The experimental maximal load was 189.2 kN, 1.4% more than the control beam. It increased 14% above the unstrengthened square-opening beam. The finite element model (FEM) anticipated a 7.7% increase in ultimate load to 203.777 kN, which matched experimental data. The strengthening increased beam load-bearing capacity and reduced square-opening weakening. The load-deflection behavior was comparable to reinforced square-opening beam studies (Hussein et al., 2020; Morsya and Barima, 2019). Though strengthening increased the total load-carrying capacity, the initial stiffness did not significantly increase in comparison with the unstrengthened specimen. This is due to the fact that the steel plate contribution is more effective once cracking has started and the initial response is dominated by the stiffness of the concrete. The same has been observed, with the response at the first stage not being significantly influenced by strengthening systems (Branesh Robert et al., 2021; Kholil and Ahmed, 2026).

The specimen SOS exhibited a modification in the fracture pattern behavior after strengthening. Several fractures propagated over the reinforced region, and were often more vertical, which is characteristic of flexural behaviour. But the major fracture was not exactly kept parallel to the reinforced area, but deviated a little from the edge of steel plate. This is explained by the redistribution of stresses owing to the steel plate which increased the stiffness of the strengthened region and moved the critical tensile stresses in the concrete to the surrounding unstrengthened concrete. Consequently, crack propagation took the path of least strength outside the strengthened zone as is also the case with beams strengthened around openings where cracks are likely to avoid the strengthened zone. In addition, the square opening had sharp edges, which still influenced the local stress field. The maximum deflection was 19.3 mm which is less than the control beam and the opening beam without reinforcement. The increase in ultimate load enhancement and the little loss of deformation capacity is consistent with previous studies on strengthened beams (Almusallam et al., 2018; Hussein et al., 2020). In addition, the bonding failure between the surface of steel plate and beam did not occur during the test indicating that the strengthening system was capable of transmitting the load without premature failure of the connection (Kholil and Ahmed, 2026).

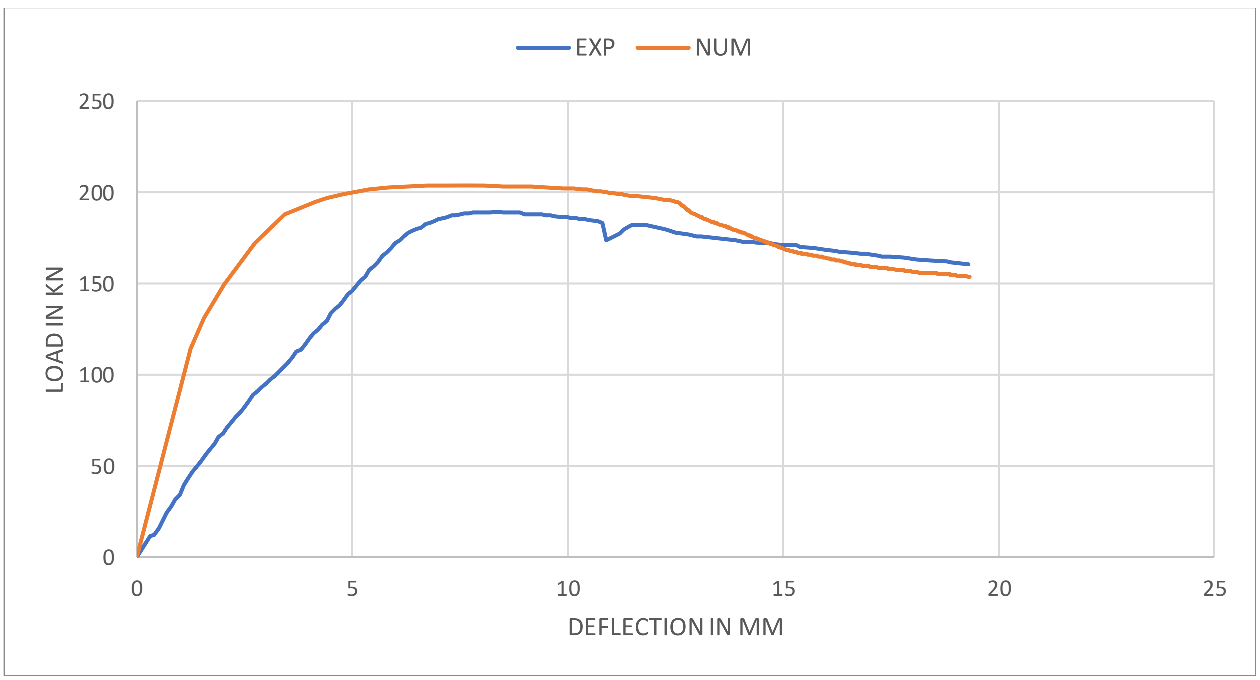

Figure 9. Load–Deflection Curve for SOS sample

Beam with Rectangle opening (RO)

The introduction of the opening led to the ultimate load of specimen RO being reduced by 11.7% relative to that of the control beam, reaching 164.7 kN as shown in Figure 10. The finite element model, however, estimated a load that was about 12.5% higher than the experimental load, reaching 185.206 kN. The load-deflection behavior of specimen RO had a lower initial stiffness compared to the control beam, which implies that the rectangular opening undermined the beam response at the initial stages of loading. This is attributed to the fact that the internal force paths are disturbed by the existence of the opening, which causes stress concentration at the edges of the opening, as observed in previous studies on beams with openings (Almusallam et al., 2018; Hussein et al., 2020; Morsya and Barima, 2019). Cracking began at the bottom tension zone and then extended upwards to the opening area. Although the failure mode was predominantly flexural, the rectangular opening changed the crack path. Due to the effect of the rectangular opening on the internal force flow and stress field, the main crack tended towards the opening and did not follow a vertical path. This is consistent with previous studies on beams with openings where the cracks are diagonal due to stress concentration (Hussein et al., 2020; Morsya and Barima, 2019).The final deflection was less than that of the control beam, reaching 20.7 mm. Overall, the existence of the rectangular opening resulted in a lower structural response, with lower stiffness, load-carrying capacity, and ductility, and enhanced faster crack propagation in the opening area, as also observed in earlier work where openings decreased stiffness, load capacity, and ductility (Almusallam et al., 2018; Hussein et al., 2020).

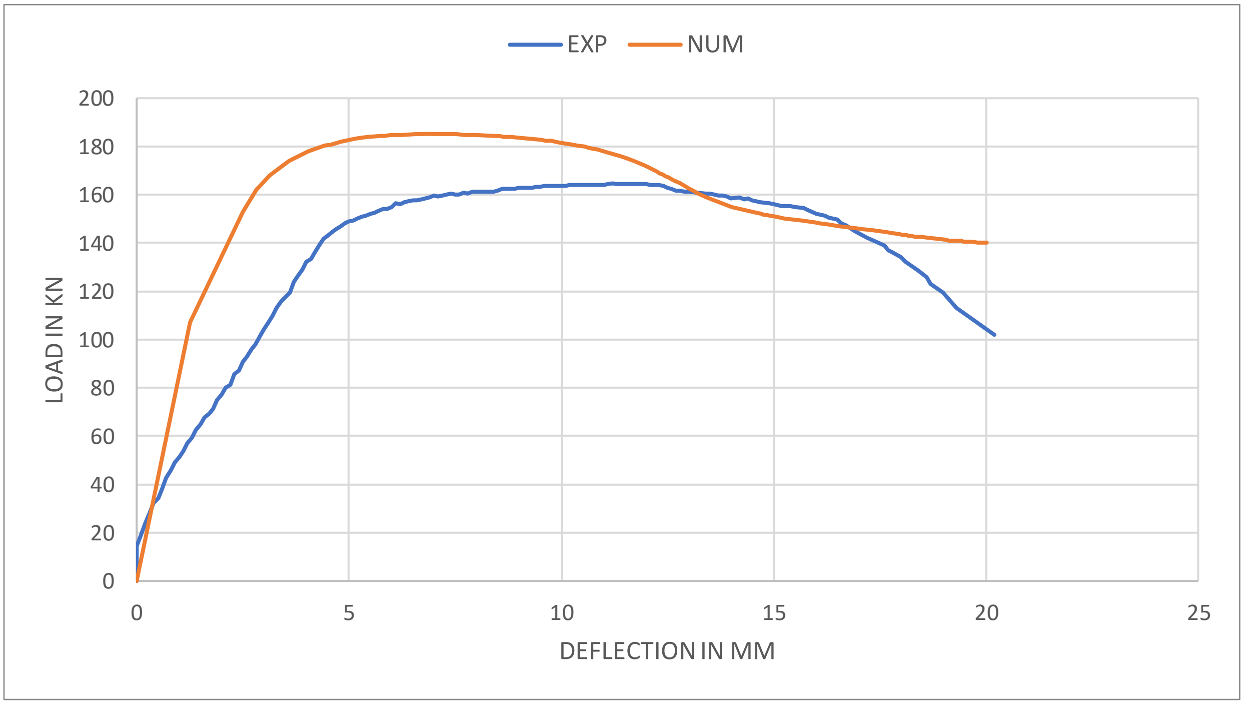

Figure 10. Load–Deflection Curve for RO sample

Beam with rectangular opening Strengthened using Steel Plate (ROS)

Strengthening of the rectangular opening with external steel plates enhanced the structural response of specimen ROS as shown in Figure 11. The maximal load of the experiment was 172.1 kN that is more than the unstrengthened rectangular specimen but less than control beam. This means the strengthening system was able to recoup some of the load bearing capacity lost owing to the opening, but not all of the original capability. This discovery is consistent with the past study findings that strengthening improved the structural behavior but not necessarily the complete capacity of members with openings (Ghani and Izzet, 2025; Kamal and Hosny, 2011). The ultimate load of 200.142 kN was predicted by the finite element model, which is greater than the experimental outcome and the numerical prediction of the control beam. This is indicative of the fact that the numerical model is biased towards overestimating the strengthening effect, but the general trend is similar to the behavior in the experiment. The load-deflection curve indicated that the stiffness was improved over the unstrengthened specimen, and the behavior was similar to that of the control beam in the early loading stages. The strengthening using steel plates helped in redistribution of stress and increased the stiffness of the beam resulting in a more stable performance at the point of failure as observed in other studies (Ghani and Izzet, 2025). The final deflection was about 20 mm and was slightly less than that of the unstrengthened specimen. This implies that the strengthening was accompanied by a decrease in the deformation capacity, which is usually witnessed in externally strengthened members owing to the corresponding rise in stiffness (Kamal and Hosny, 2011).

After strengthening, there was a change in the crack pattern. The majority of cracks were almost vertical, which meant that flexural behavior was reverted to. The crack that formed was the dominant one, which started at the bottom tension zone and spread upwards to the compression region in an almost vertical direction. The distribution of the cracks was however not completely symmetric, with a stronger crack being found on one side of the opening. The differences in crack patterns are postulated to be caused by local material properties and fiber distribution, although the strengthening system is advantageous. Although strengthening can alter crack paths, it does not eliminate stress concentrations at sharp corners (Chkheiwer and Abdullah, 2017). The connection between the concrete surface and the steel plates was not lost during the loading process, which proves the effectiveness of the system and confirms the results of earlier research on debonding failure prevention (Kamal and Hosny, 2011).

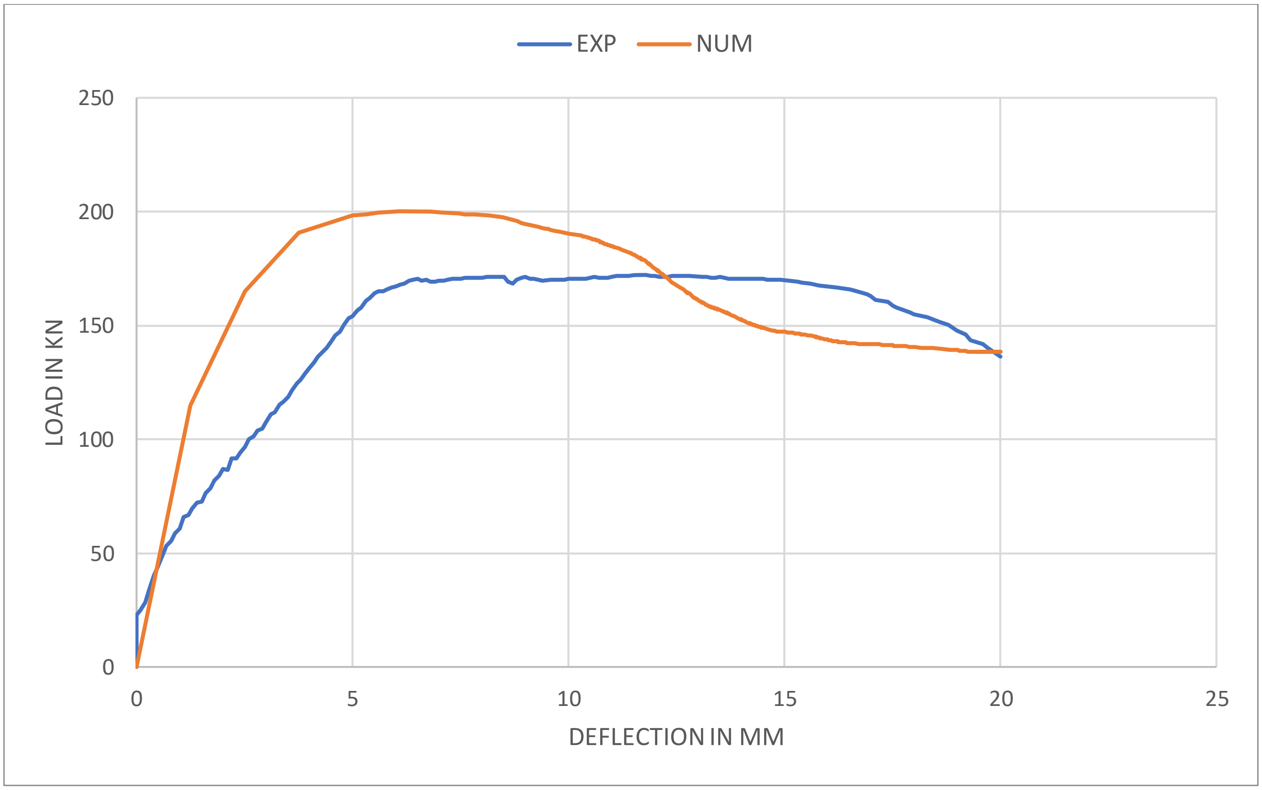

Figure 11. Load–Deflection Curve for ROS sample.

Effect of Opening

Web openings were found to have a definite effect on the structural behavior of the tested UHPC beams. Internal forces were evenly distributed across the cross-section in the control beam. Nevertheless, the existence of square and rectangular openings caused geometric discontinuities which disturbed the internal force paths and changed the distribution of stress in the beam, as was observed in earlier works (Almusallam et al., 2018; Morsya and Barima, 2019).

The square hole caused a significant decrease in structural performance. The localized stress concentrations created by the sharp edges of the opening hastened crack initiation and caused greater damage in the area of the opening. This was observed in the decrease in the cracking load and ultimate load as compared to the control beam. Moreover, the crack pattern was not simply vertical, which indicates the influence of the opening on internal force distribution (Hussein et al., 2020; Morsya and Barima, 2019).

The effect was more pronounced in the rectangular opening specimen. Besides the concentration of stresses at the corners, the long shape of the opening also disrupted the flow of internal forces in the beam. Consequently, the rectangular opening had a large decrease in load-carrying capacity relative to the other specimens. This also affected the deformation behavior, with more severe cracking observed in the area around the opening (Almusallam et al., 2018; Hussein et al., 2020).

Mechanically, the observed behavior may be explained by the change in the routes of stress flow in the beam. The natural distribution of stresses is disrupted in the presence of square and rectangular openings and stresses are redirected around the boundaries of openings, which leads to local tensile concentrations, especially at the corners leads to faster crack initiation and more disrupted crack propagation pattern than control beam, which is in agreement with the results of other studies (Morsya and Barima, 2019). The crack patterns of the experimental specimens confirm this interpretation. The square and rectangular openings created inclined crack paths around the opening area, which is an indication of stress concentration and disruption of stress distribution in the area of the opening. This implies that the geometry of the opening influences the extent of stress concentration as well as the position and formation of cracks in the beam (Hussein et al., 2020). In general, the findings indicate that the introduction of openings causes a decrease in structural performance, such as a decrease in stiffness and load-carrying capacity (Almusallam et al., 2018). The rectangular opening was found to have a more severe effect on the strength and cracking behavior than the square opening among the investigated configurations (Morsya and Barima, 2019). These results underscore the need to take into account the shape of openings in the design of UHPC beams, particularly when the openings are in the flexural region.

Effect of Steel Plate Strengthening

The external steel plate strengthening was found to have a demonstrable effect on the structural performance of the UHPC beams with square and rectangular apertures. In general, the strengthening system was effective in reducing the negative effects of openings by minimizing stress concentration and localized damage in the vicinity of the apertures as found in previous studies of reinforced beams with openings (Hussein et al., 2020; Kholil and Ahmed, 2026; Morsya and Barima, 2019). The steel plate helped to slow crack initiation, as the increased cracking loads of the strengthened specimens compared to the unstrengthened ones indicate. This is due to the fact that the addition of local stiffness (steel plate) allowed minimizing tensile strains in the most problematic areas and reducing stress concentration, especially around the edges of the openings (Hussein et al., 2020; Morsya and Barima, 2019).

The response of the two specimens differed. The strengthened square opening specimen showed a complete recovery and slight increase beyond the capacity of the control beam, as compared to the rectangular specimen that only attained partial recovery because of the more drastic disturbance of stress flow that is inherent in its geometry (Hussein et al., 2020; Kamal and Hosny, 2011). The load-deflection curves indicate that the strengthening system is most effective after crack formation and close to the ultimate load. The rectangular specimen demonstrated a significant stiffness increase, but the square specimen demonstrated a small initial elastic response, which is in line with previous results that indicate strengthening systems have more influence on the post-cracking structural response (Branesh Robert et al., 2021).

The strengthening system was an external tensile reinforcement that assisted in stress redistribution and reduction of tensile damage around the openings. The shape of the opening also affected stress redistribution, and sharp corners and long openings were known to affect stress redistribution (Almusallam et al., 2018; Morsya and Barima, 2019). The crack patterns were also a good indicator of this behavior; strengthening led to the change in crack paths to the edges of the openings, which was an indication of a change in stress distribution. The rectangular specimen had more vertical flexural cracks than the square specimen, which had inclined cracks due to stress concentration at the corners. These observations suggest that while strengthening can change crack patterns and improve stress redistribution, the effect of geometric discontinuities is still present (Hussein et al., 2020).

Second, fractures spread into the concrete around stronger parts, not into them. Steel plates transferred pressures away from the aperture to protect the weakest portions, as shown in reinforced beams where fractures are improbable (Hussein et al., 2020). Finally, the tests showed no debonding, confirming that the link between the steel plate and the concrete surface was strong enough to transmit stresses (Kholil and Ahmed, 2026).

Failure Modes and Crack Patterns

This study carried out loading tests on UHPC beams with varied opening conditions and reinforcement configurations and verified the reliability of the numerical simulation method adopted. The failure characteristics of all test specimens differed significantly as shown in Figure 12 (a-b). The non-opening control beam CB was employed as a reference, and showed conventional flexural failure. Vertical fractures first appeared at the bottom of the tensile zone at the midspan constant bending force area, and then propagated progressively to the compression zone. SO, an unreinforced opening-group specimen with a square aperture, showed oblique-flexural fractures pointing towards the corners of its opening. The rectangular-opening specimen RO, whose opening was more elongated, suffered more severe disruption to its stress flow path. Its crack inclination and degree of localization were far higher than those of SO. Both kinds of opening beams produced long oblique fractures and local tensile damage at the opening borders due to load concentration and broken internal force transmission. Specimens SOS and ROS externally joined with steel plates showed more appropriate fracture redistribution and more stable flexural behavior. The cracks of these specimens propagated mostly in the vertical plane and clustered outside the reinforced zone. The SOS specimen showed evenly distributed fractures in its opening area while the ROS specimen performed more excellent in crack control and delay of damage. The numerical damage contours derived in this investigation by applying the concrete damage plasticity (CDP) model agreed well with the actual crack patterns. The model can well describe the start, propagation and localization of tensile damage throughout the whole loading process, which can demonstrate the dependability of this nonlinear finite element approach.

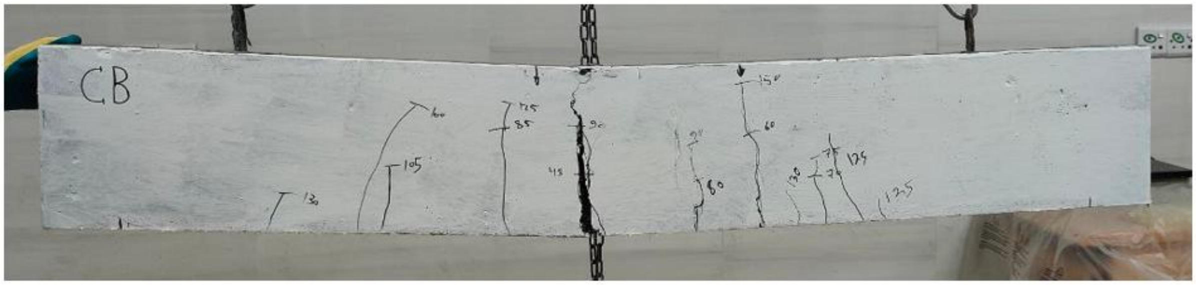

(a)

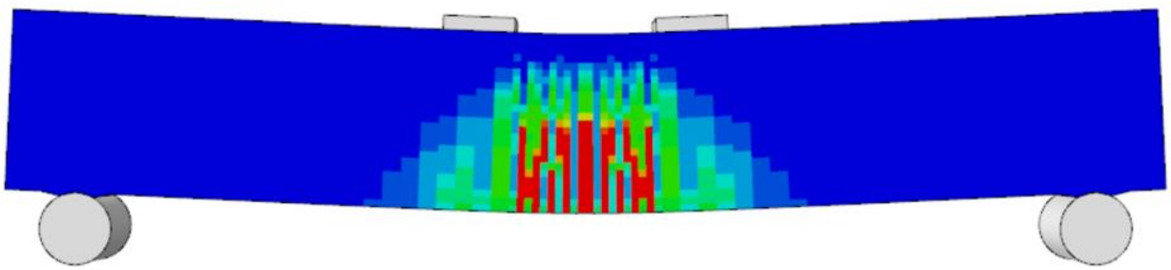

(b)

Figure 12. Experimental crack pattern and numerical damage prediction for the control beam (CB): (a) experimental result and (b) numerical result

(a)

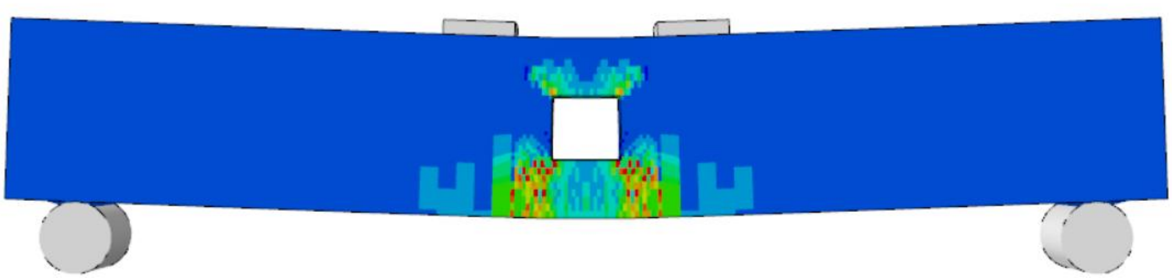

(b)

Figure 13. Experimental crack pattern and numerical damage prediction for the beam with an opening (SO): (a) experimental result and (b) numerical result

In the beams with openings (SO and RO), the bottom tension zone was also the source of cracking, but it was influenced by the existence of the openings as shown in Figures 13(a-b) and 14(a-b). The main crack was inclined towards the opening. This implies that the internal force paths change and stress concentrations are formed, especially at the edges and corners of the openings, as has been reported in earlier studies (Almusallam et al., 2018; Hussein et al., 2020; Morsya and Barima, 2019). These beams had a higher inclination of cracks, which indicated greater disruption of the stress distribution.

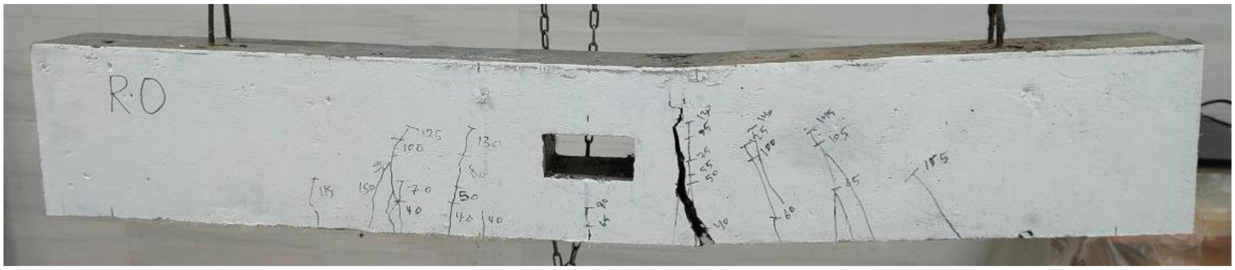

(a)

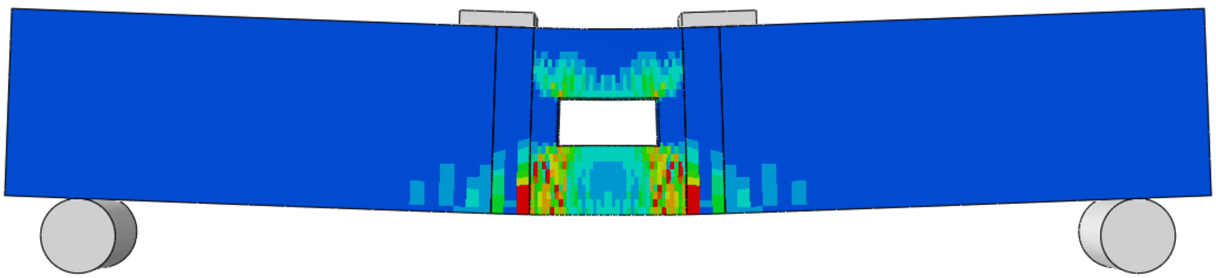

(b)

Figure 14. Experimental crack pattern and numerical damage prediction for the beam with an opening (RO): (a) experimental result and (b) numerical result

(a)

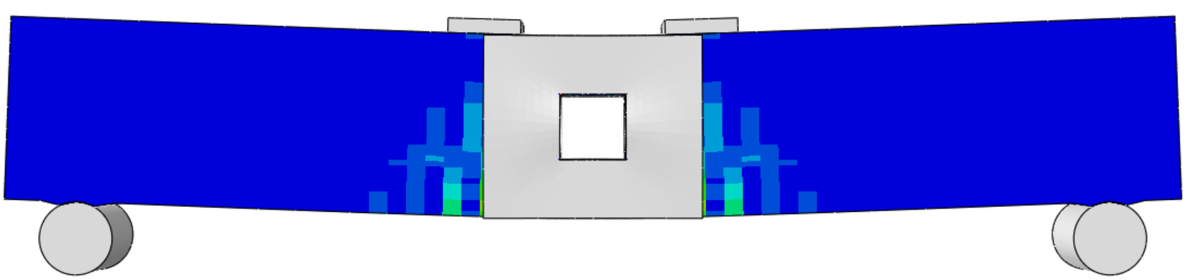

(b)

Figure 15. Experimental crack pattern and numerical damage prediction for the beam with an opening (SOS): (a) experimental result and (b) numerical result

Cracks still initiate from the lower tension zone in the strengthened specimens (SOS and ROS) as shown in Figures 15(a-b) and 16(a-b), but the crack path becomes more vertical than in the unstrengthened specimens, suggesting better stress redistribution after strengthening (Almusallam et al., 2018). The crack path in the SOS specimen was slightly inclined due to the effect of the sharp corners, which still affected the local stress distribution after strengthening. However, the ROS specimen showed a more vertical flexural crack pattern. Strengthening systems change crack paths and return the behavior to flexural without removing the effect of the geometry, which agrees with previous research (Hussein et al., 2020).

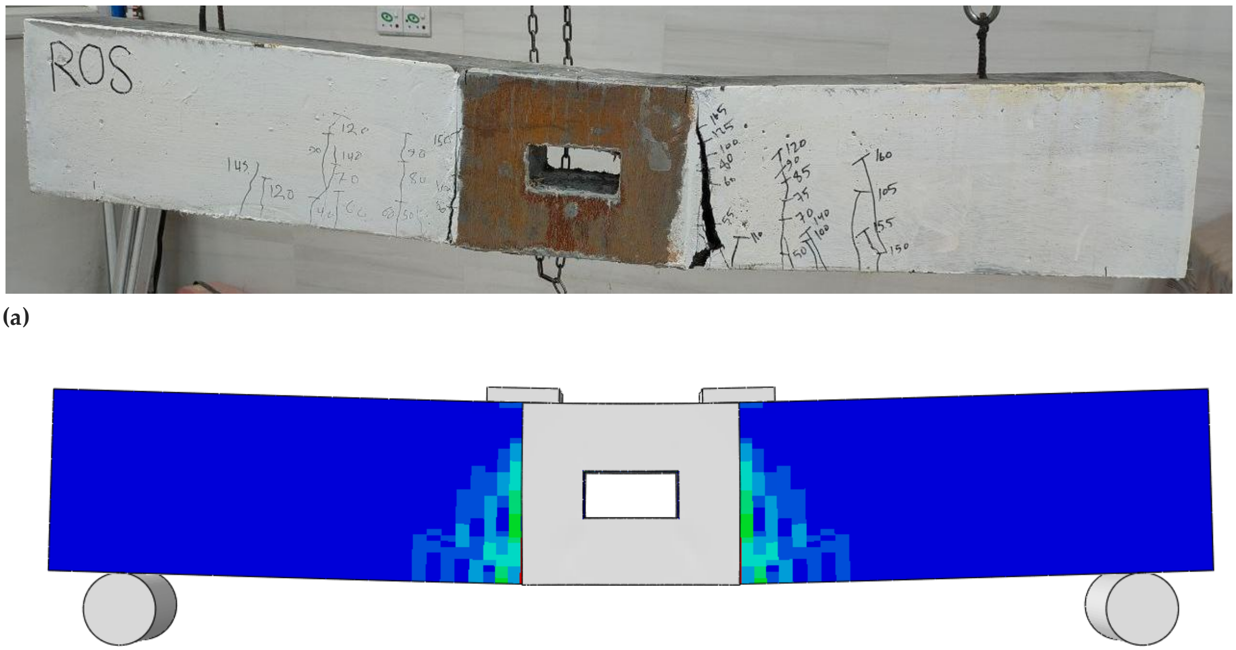

(a)

(b)

Figure 16. Experimental crack pattern and numerical damage prediction for the beam with an opening (ROS): (a) experimental result and (b) numerical result

In all the strengthened specimens, the cracks did not extend through the strengthened areas but rather formed in the concrete around them. This shows that the steel plate was able to redistribute stresses at the opening and shield the weakened area, as is also the case with strengthened beams where cracks are likely to avoid strengthened areas (Hussein et al., 2020). There was no evidence of debonding between the concrete surface and the steel plate, indicating that the bond performance was satisfactory and that stress was transferred to the concrete surface during loading, which is consistent with other literature on externally strengthened members (Kamal and Hosny, 2011).

Numerical vs Experimental

This study develops a nonlinear finite element model for UHPC beams with transverse openings and external steel plate reinforcement, to verify the model's reliability. First, the ultimate load-carrying capacity predictions output by the model are compared with the measured experimental values of five types of test specimens: CB, SO, SOS, RO, and ROS. Results demonstrate that all forecast values are somewhat higher than the actual measured values with errors of 6.3%, 12.1%, 7.7%, 12.5% and 16.3% for each specimen accordingly. However, the magnitude of divergence is still within the permitted range for nonlinear numerical simulations of UHPC members (Taher 2024; Kholil and Ahmed, 2026). The causes of the overestimation can be grouped into two categories. First, the idealized modeling assumptions of the finite element model, including the assumption of perfect bonding between materials and simplified treatment of UHPC's constitutive behavior, led to an overestimated model stiffness. Second, interference factors occurred during the experimental stage, such as construction defects, material heterogeneity, and uncertainty in boundary conditions. This model can represent six major structural reactions properly, i.e. load-deflection behavior, overall stiffness degradation, crack starting zone, post-peak behavior, effect of opening shape and efficiency of steel plate reinforcing. Their outputs agree well with the reported experimental behavior. Therefore, the model may be used as a trustworthy tool to forecast the structural behavior of comparable UHPC beams.

4. CONCLUSION

This paper examined the structural performance of ultra-high-performance concrete (UHPC) beams with square and rectangular web openings by experimental testing and nonlinear finite element analysis, as well as the performance of external steel plate strengthening.

1. The presence of square and rectangular openings resulted in a decrease in the ultimate load capacity because of disruption of internal force flow and the development of local tensile damage. The decrease was greater in rectangular openings than in square openings.
2. Although the strength decreased, all specimens showed stable post-peak behavior without brittle failure. This is due to the improved tensile behavior of UHPC and the fiber-bridging mechanism.
3. External steel plate strengthening greatly enhanced the structural performance of the beams. The strengthened square opening specimen could recover and slightly surpass the capacity of the control beam, but the strengthened rectangular specimen exhibited partial recovery.
4. The strengthening system served to delay the crack start, reduce the stress concentrations at the apertures and improve the stress redistribution. The fracture patterns moved to a more flexural mode after strengthening, however certain aberrations still occurred depending on the opening geometry
5. The finite element model was found to be in good agreement with the experimental results in overall structural behavior, such as load-deflection response and crack development. Nevertheless, the model slightly overestimated the ultimate load capacity because of idealized assumptions.
6. The CDP model and cohesive surface interaction provided a good representation of the behavior of UHPC beams with openings and external strengthening.

Acknowledgement

We thank University of Babylon and laboratory staffs who help me to complete the experimental work.

Author Contributions

Hayder S.H. Hudaib: was conducted the experimental work and write the draft manuscript; Hayder M.J. Al-Khafaji conducted the discussion of the results and revised manuscript final draft.

Ethical issues

Not applicable. This study does not involve any experiments on humans or animals. Hence, ethical approval was not required.

Informed consent

Not applicable.

Funding

This research did not receive any external funding like specific grant from funding agencies in the public, commercial, or nonprofit sectors.

Conflict of Interest

The authors declare that they have no conflicts of interest, competing financial interests or personal relationships that could have influenced the work reported in this paper.

Data and materials availability

All data associated with this study will be available based on the reasonable request to corresponding author.

REFERENCES

1. Adhikary BB, Mutsuyoshi H. Numerical simulation of steel-plate strengthened concrete beam by a non-linear finite element method model. Constr Build Mater 2002; 16(5):291–301. doi:10.1016/S0950-0618(02)00022-3
2. Al-Enezi MS, Yousef AM, Tahwia AM. Shear capacity of UHPFRC deep beams with web openings. Case Stud Constr

Mater 2023; 18:e02105. doi:10.1016/j.cscm.2023.e02105
3. Almusallam T, Al-Salloum Y, Elsanadedy H, Alshenawy A, Iqbal R. Behavior of FRP-strengthened RC beams with large rectangular web openings in flexure zones: experimental and numerical study. Int J Concr Struct Mater 2018; 12(1). doi: 10.1186/s40069-018-0272-5
4. Al-Sheikh SA. Flexural behavior of RC beams with opening. Concr Res Lett 2014; 5(2):812–824.
5. Andoh G, Kankam CK, Ohene-Coffie F, Nanor ES, Kpo SAK, Sarpong KO, Issifu FA. Flexural behavior of reinforced concrete beams with openings created by PVC pipes: an experimental and numerical study. Asian J Adv Res Rep 2025; 19(1):252–269. doi:10.9734/AJARR/2025/v19i1879
6. Aykac B, Kalkan I, Aykac S, Egriboz YE. Flexural behavior of RC beams with regular square or circular web openings. Eng Struct 2013; 56:2165–2174. doi:10.1016/j.engstruct.2013.08.043
7. Branesh Robert J, Angeline Prabhavathy R, Joanna PS, Christopher Ezhil Singh S, Murugan S, Rajkumar S, Sharma S. Flexural behaviour of RC beams with a circular opening at the flexural zone and shear zone strengthened using steel plates. Adv Civ Eng 2021; 2021:6733402. doi:10.1155/2021/6733402
8. Chkheiwer AH, Abdullah MD. Flexural behavior of high strength RC slabs with opening strengthening with wire mesh and steel fibers. Kufa J Eng 2017; 8(3):103–118. doi:10.30572/2018/KJE/8031156
9. Fakeh M, Jawdhari A, Fam A. Recommended concrete damage plasticity parameters and constitutive models for UHPC in ABAQUS. Eng Struct 2025; 333:120154. doi:10.1016/j.engstruct.2025.120154
10. Ghani HA, Izzet AF. Strengthening reinforced concrete beams vertically perforated through their entire depth with the use of steel tubes. Eng Technol Appl Sci Res 2025; 15(4):25445–25451. doi:10.48084/ETASR.11854
11. Hamoda A, Yehia SA, Ahmed M, Abadel AA, Baktheer A, Shahin RI. Experimental and numerical analysis of deep beams with openings strengthened with galvanized corrugated and flat steel sheets. Case Stud Constr Mater 2024; 21:e03522. doi:10.1016/j.cscm.2024.e03522
12. Huang Y, Yao G. Shear strength of ultra-high-performance concrete beams without stirrups: a review based on a database. Buildings 2024; 14(5):1212. doi:10.3390/buildings14051212
13. Hussein TS, Shaheed SM, Dakhil AJ. The opening presence effect on the flexural response of concrete beams. TEST Eng Manag 2020; 83(5–6):2864–2871.
14. Kadhim MMA, Jawdhari A, Peiris A. Development of hybrid UHPC-NC beams: a numerical study. Eng Struct 2021; 233:111893. doi:10.1016/j.engstruct.2021.111893
15. Kamal AY, Hosny E. Strengthening of RC beams with openings by near surface mounted CFRP: experimental study. Eng Res J 2011; 129.
16. Kartal S, Kısıklı E. Bending behavior of RC beams with regular web openings and non-corroding GFRP reinforcement. Int J Concr Struct Mater 2024; 18(1). doi: 10.1186/s40069-024-00719-3
17. Kazem ZUM, Al-Zahra BIA. Strengthening RC one way solid slab with opening using different sustainable techniques (CFRP laminates, CFRP rebars, UHPC plates). IOP Conf Ser Earth Environ Sci 2025; 1507(1):012057. doi:10.1088/1755-1315/1507/1/012057
18. Kholil MI, Ahmed A. Finite element modelling of RC beam strengthened with epoxy-bonded steel plate. J Build Pathol Rehabil 2026; 11(1):1. doi:10.1007/s41024-025-00672-y
19. Morsya A, Barima AM. Behavior of RC beams with openings using different strengthening techniques. Int J Sci Basic Appl Res 2019; 46(1):195–219.
20. Özkılıç YO, Aksoylu C, Hakeem IY, Özdöner N, Kalkan İ, Karalar M, Stel'makh SA, Shcherban EM, Beskopylny AN. Shear and bending performances of reinforced concrete beams with different sizes of circular openings. Buildings 2023; 13(8):1989. doi:10.3390/buildings13081989
21. Richard P, Cheyrezy M. Composition of reactive powder concretes. Cem Concr Res 1995; 25(7):1501–1511. doi:10.1016/0008-8846(95)00144-2
22. Sathiyapriya D, Suganya Devi K, Sattainathan Sharma A. Study on flexural behaviour of reinforced concrete beam with effective openings. J Phys Conf Ser 2021; 2040(1):012030. doi: 10.1088/1742-6596/2040/1/012030
23. Taher AM. Nonlinear finite-element analysis of RC beams with various opening near supports. Open Eng 2024; 14(1). doi:10.1515/eng-2024-0074
24. Yang J, Chen B, Su J, Xu G, Zhang D, Zhou J. Effects of fibers on the mechanical properties of UHPC: a review. J Traffic Transp Eng (Engl Ed) 2022; 9(3):363–387. doi:10.1016/j.jtte.2022.05.001
25. Zhu Y, Shi T, Zhu Y, Zhu Z, Wang K. Analysis on flexural performance of prestressed steel-reinforced UHPC beams. Buildings 2024; 14(12):4029. doi:10.3390/buildings14124029
26. Zhu Y, Zhang Y, Yuan X, Hou C. An adaptive crack width prediction for flexural steel reinforced UHPC beams. Int J Concr Struct Mater 2023; 17(1):73. doi:10.1186/s40069-023-00628-x